JOURNAL OF AIRCRAFT
Vol. 44, No. 6, November–December 2007

Upstream Blowing Jet on Transonic Convex-Corner Flow

Kung-Ming Chung*
National Cheng-Kung University, Tainan 711, Taiwan, Republic of China

DOI: 10.2514/1.32203

The present study investigates the effects of an upstream blowing jet on the compressible convex-corner flows. The characteristics of mean and fluctuating pressure distributions are associated with the type of expansion flows, blowing rates, and porosity. Even a small amount of upstream blowing tends to delay the transition of subsonic and transonic expansion flows, thus reducing the levels of downstream surface pressure fluctuations in subsonic interactions. The intensity of surface pressure fluctuations is associated with blowing rates for the separated flows. Larger blowing rates result in upstream movement of shock wave and enhance the flow unsteadiness (or peak surface pressure fluctuations) near the corner.

Nomenclature

B, B_d	=	blowing parameter
C_p	=	pressure coefficient, $(p_w - p_\infty)/q_\infty$
C_{σ_p}	=	pressure fluctuation coefficient, $(\sigma_{p,w} - \sigma_{p,\infty})/q_\infty$
M	=	freestream Mach number
M_1	=	local Mach number upstream of shock
p_w	=	surface static pressure
q_∞	=	freestream dynamic pressure
x	=	coordinate along the surface of the corner
x^*	=	x/δ
δ	=	incoming boundary layer thickness
η	=	deflected angle, in degree

I. Introduction

DEFLECTED flaps can be used as the high-lift device to obtain the maximum performance of an aircraft, which is associated with the variable camber control within the operational flight envelope [1]. At cruise speeds, the benefits of a variable camber using a simple trailing-edge control surface could approach more than 10% in maximizing the lift-to-drag ratio, especially for nonstandard flight conditions. However, there is a great uncertainty regarding the allowable device deflection with the critical Mach number, the onset of the boundary layer separation, and drag. In particular, the local flow conditions around the convex corner are of importance in determining the efficiency of a deflected control surface [2]. Chung [3] indicated that a compressible convex-corner flow shows a mild initial expansion, a strong expansion near the corner, and a downstream recompression. Transition of the subsonic and transonic expansion flow and the interaction region can be scaled with the freestream Mach number and the convex-corner angle ($M^2\eta$). The small separation bubble may be borne at the formation of a normal shock wave [4], and an extensively separated region is observed at $M^2\eta \geq 8.95$ [5]. The separation position moves slightly upstream while the reattachment position moves downstream with increasing convex-corner angle. The measurements of surface pressure fluctuations indicate the intermittent nature of the pressure signals, and the amplitude of peak pressure fluctuations could also be scaled with $M^2\eta$. The unsteadiness of the flow is related to the type of expansion flow and the shock wave excursion phenomena.

Presented as Paper 2005-0644 at the 43th AIAA Aerospace Sciences Meeting and Exhibit, Reno, Nevada, 10–12 January 2005; received 17 May 2007; revision received 2 August 2007; accepted for publication 2 August 2007.

*Research Fellow, Aerospace Science and Technology Research Center.

The boundary layer blowing has been employed to suppress the shock-induced separation [6]. A localized blowing system can be used in place of vortex generators to alleviate the effects of shock wave/boundary layer interactions. In addition, blowing is qualitatively equivalent to a decrease in Reynolds number. Injection of a small quantity of high-pressure air upstream of the shock can energize the incoming boundary layer, thus inducing the increase in displacement thickness (less fuller boundary layer) [7]. Fernandez and Zukoski [8] indicated that the effectiveness of blowing is related to the rates of injection. Lower mass injections produce only modest effects on the boundary layer profile or the freestream flow, whereas very large rates of injection may cause separation of the injected mass and the boundary layer. In the current study, the main purpose is to evaluate the effectiveness of the upstream blowing jet on the shock-induced separation and the associated fluctuating pressure load. This investigation involved the analysis of mean and fluctuating pressure distributions of the convex-corner flows with low to mild upstream boundary layer blowing.

II. Experiment

A. Transonic Wind Tunnel

The Aerospace Science and Technology Research Center/National Cheng-Kung University (ASTRC/NCKU) transonic wind tunnel is a blowdown type and operates in the Mach number from 0.2 to 1.4 at Reynolds numbers up to 20×10^6/m [9]. Major components of the facility include compressors, air dryers, a cooling water system, storage tanks, and the tunnel. The dew point of the high-pressure air through the dryers is maintained at −40°C under normal operation conditions. Air storage volume for the three storage tanks is up to 180 m^3 at 5.15 MPa. The test section is 600 × 600 mm and 1500 mm long. In the present study, the test section has a combination of solid sidewalls and perforated top/bottom walls to reduce the background acoustic noise. The freestream Mach numbers were 0.64 and 0.83 ± 0.01. The stagnation pressure p_0 and temperature T_0 were 172 ± 0.5 kPa and ambient temperature, respectively.

For the data acquisition system, the test conditions were recorded by the NEFF Instrument Corporation system while the LeCroy 6810 waveform recorders were used for the pressure measurements. A host computer with CATALYST software controlled the setup of LeCroy waveform recorders through a LeCroy 8901A interface. All input channels were triggered simultaneously using an input channel as the trigger source. The output range of waveform recorders was adjusted for an optimum resolution, and the relative error of the mean pressure signals is estimated to be about 0.1%.

B. Test Model

The test model consists of a flat plate, a perforated plate, and an interchangeable instrumentation plate, as shown in Fig. 1a. The test model is 150 mm wide and 600 mm long and is supported by a single sting mounted on the bottom wall of the test section. The high-pressure air was injected through the perforated plate, as seen in

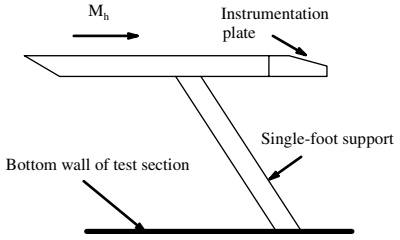

a) Test model

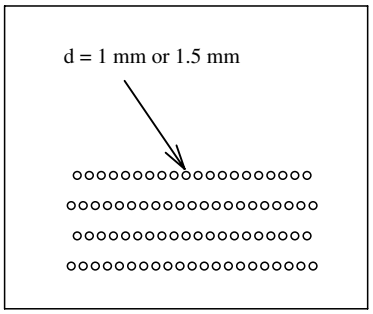

b) Perforated plates

Fig. 1 Test configuration.

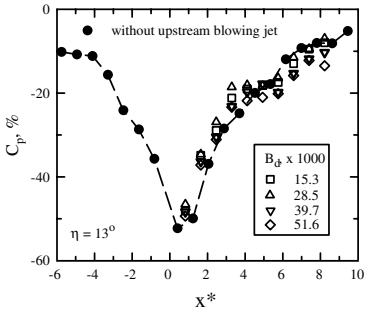

a)

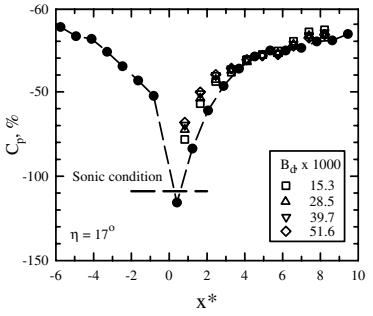

b)

Fig. 2 Pressure distributions, $M = 0.64$ (plate 1, 4% porosity).

Fig. 1b. Plate 1 had 82 uniformly distributed normal holes with a diameter of 1.0 mm. Plate 2 is the same as plate 1 except that the holes have a diameter of 1.5 mm. The holes (5 mm apart) were uniformly distributed in four rows, and the last row was located at 7 mm upstream of the convex corner. The blowing jet was supplied from a plenum underneath connected to the high-pressure air tank through an 8-mm pipe. The 13-, 15-, or 17-deg convex corner is located at 500 mm from the leading edge of the flat plate. Ten flush-mounted pressure transducers were installed along the centerline of each instrumentation plate perpendicular to the test surface. Side fences were installed on the instrumentation plate to prevent cross flow from the underside of the plate.

C. Experimental Technique

The Kulite (Model XCS-093-25A, B screen) pressure transducers were powered by a Topward Electronic System (TES Model 6102) power supply at 15.0 V. The outer diameter is 2.36 mm, and the sensing element is 0.97 mm in diameter. External amplifiers (Ecreon Model E713) were also employed to improve the signal-to-noise ratio. The natural frequency is 200 kHz as quoted by the manufacturer. However, Gramann and Dolling [10] indicated that the perforated screen of the Kulite pressure transducers might limit the frequency response only up to 50 kHz. The sampling period is 5 μs (200 kHz) for all the test cases. Each data record contains 131,072 data points for statistical analysis. The data were divided into 32 blocks. The mean values of each block (4096 data points) were calculated. Uncertainty of the experimental data of the flat plate case was estimated to be 0.43 and 0.15% for the static pressure coefficient and surface pressure fluctuation coefficient, respectively. For the characteristics of the incoming boundary layer, Miau et al. [11] indicated that the transition of the boundary layer under the present test condition is close to the leading edge of the flat plate. The boundary layer thicknesses, in the absence of the perforated plate, at 25 mm upstream of the convex corner were estimated to be 7.3 and 7.1 ± 0.2 mm for $M = 0.64$ and 0.83, respectively. The Reynolds numbers based on the incoming boundary layer thickness (Re_δ) were 1.49 and 1.68×10^5.

A 4-mm sonic nozzle manufactured by Flow Systems (FSI) was installed to control the mass flow of the blowing jet. The rates of blowing were calculated according to the stagnation condition upstream of the sonic nozzle (Kulite pressure transducer Model XT-140-500A and temperature of the high-pressure air tank). The stagnation pressure ($p_{0,j}$) ranges from 0.3 to 1.0 MPa, and the stagnation temperature is room temperature. The blowing jet to freestream stagnation pressure ($p_{0,j}/p_0$) ratio is up to 5.8. Injection was taking place over two-thirds width of the perforated plate (100-mm wide). Two blowing parameters (B and B_d) were used as a measure of nondimensional mass injection, in which

$$B = \frac{\rho_j U_j}{\rho_\infty U_\infty} \quad \text{and} \quad B_d = \frac{\rho_j U_j A_j}{\rho_\infty U_\infty A_{j\text{-dis}}}$$

B_d is equal to B multiplied by the ratio of the injection area to the area contained within the perimeter of a rectangle which just circumscribes all the injection holes [12]. In the present situation, the blowing parameter B ranges from 0.155 to 1.295 ± 0.005. The porosity (area ratios, $A_j/A_{j\text{-dis}}$) was 4 and 8.9% for plates 1 and 2, respectively.

III. Results and Discussion

A. Mean Surface Pressure Distributions

A given amount of upstream blowing jet is expected to affect the pressure gradient and displacement thickness upstream of a convex corner. For the subsonic expansion flow ($M = 0.64$, $\eta = 13$ deg), the mean surface pressure distribution is shown in Fig. 2a. The origin of the x coordinate is at the corner. The flow accelerates upstream of the corner followed by downstream recompression. With the upstream blowing jet (plate 1, 4% porosity), the flow remains at the subsonic condition. Slightly higher levels of mean surface pressure are observed immediately downstream of the corner. This corresponds to less expansion (or lower local Mach number) near the corner. The initial compression is roughly the same at all blowing rates, and slightly lower levels of downstream pressure are associated with higher B_d. Furthermore, Inger and Zee [7] indicated that transonic interactions are very sensitive to changes in the incoming turbulent boundary layer. At $M = 0.64$ and $\eta = 17$ deg (transonic convex-corner flow), the flow without an upstream blowing jet is expanded to supersonic speed near the corner, Fig. 2b. The effect of the blowing jet is observed near the corner with higher levels of mean surface pressure, particularly with increasing B_d. This implies that the upstream blowing jet tends to reduce the streamwise extent of the interaction. The flow remains at the subsonic condition for all the test cases, which correspond to the delay in the transition of subsonic and transonic expansion flow. For the separated convex-corner flows ($M = 0.83$, $\eta = 13$ deg, and 4% porosity), the upstream blowing jet

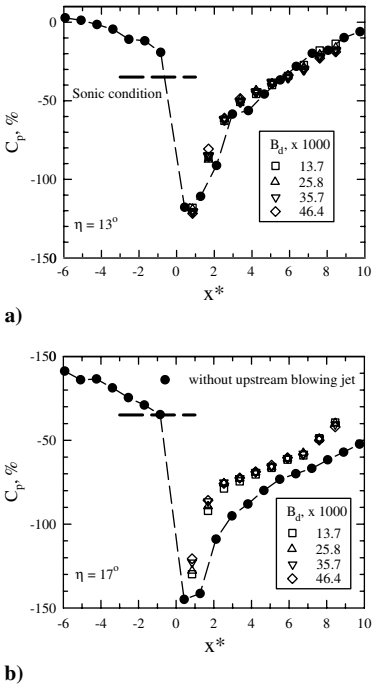

Fig. 3 Pressure distributions, $M = 0.83$, (plate 1, 4% porosity).

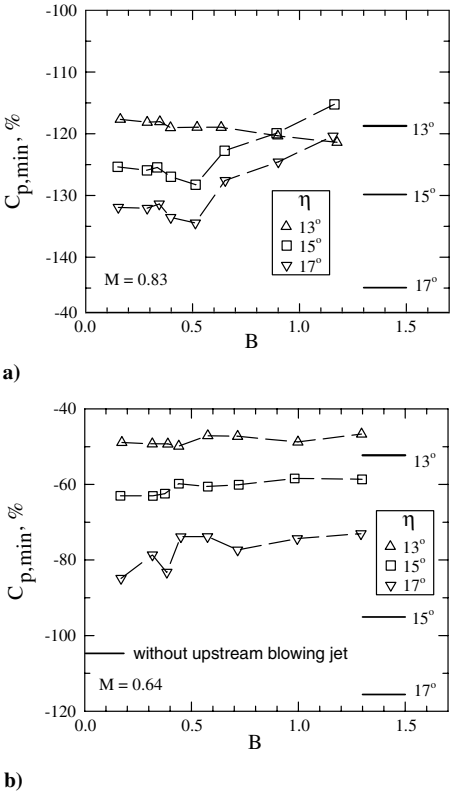

Fig. 4 Downstream expansion.

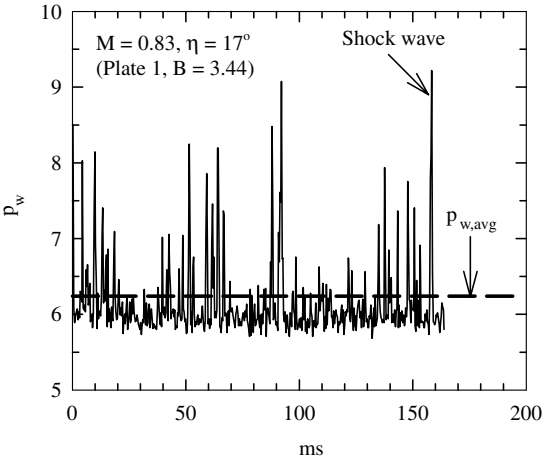

Fig. 5 Pressure–time history downstream of the convex corner.

has limited effects on the downstream mean surface pressure, seen in Fig. 3a. However, there is a higher adverse pressure gradient (initial compression) near the corner with increasing B_d. At $\eta = 17$ deg, shown in Fig. 3b, higher levels of the downstream mean surface pressure are observed. This is due to the upstream movement of the shock wave, which is also observed by the surface pressure signals. Furthermore, the effect of blowing rates on the initial compression is less pronounced with the 8.9% perforated plate.

The minimum mean surface pressure $C_{p,\min}$ near the corner is related to the upstream expansion and initial downstream compression process. Chung [3] indicated that the $C_{p,\min}$ values can be scaled with the parameter $M^2\eta$. It means that stronger expansion or higher peak Mach number is coupled with increasing Mach number and convex-corner angle. Results of the upstream blowing jet on $C_{p,\min}$ values in terms of blowing parameter B are illustrated in Fig. 4. In subsonic interactions ($M = 0.64$), there is a slight increase in $C_{p,\min}$ with increasing blowing rate B. The upstream blowing jet results in higher levels of $C_{p,\min}$, particularly at $\eta = 15$ and 17 deg. Inger and Zee [7] indicated that the blowing is qualitatively equivalent to a decrease in Reynolds number (or increasing displacement thickness upstream of the corner). This implies that the upstream expansion near a convex corner is less pronounced with decreasing Reynolds number in subsonic interactions. At $M = 0.83$ and $\eta = 13$ deg, the $C_{p,\min}$ values decrease with increasing B. There is stronger expansion near the corner at higher blowing rates. For separated convex-corner flows ($M = 0.83$, $\eta = 15$ and 17 deg), the $C_{p,\min}$ values decrease with B and reach the minimum at $B \approx 0.5$. At higher blowing rates, the large-amplitude disturbances associated with upstream movement of the shock wave result in higher levels of $C_{p,\min}$.

The shock-induced separation at transonic speeds is associated with the peak Mach number. For a circular-arc model, the critical peak Mach number does not change very much with the surface curvature (δ/R) and is close to 1.30 [13]. For the present study, the instantaneous wall pressure in transonic interactions is highly intermittent as shown in Fig. 5. The wall pressure jumps randomly back and forth, which is the superposition of fluctuations of very large amplitude on the undisturbed pressure signal. The time-averaged value of intermittent pressure signals ($C_{p,\min}$) does not correspond to the real peak Mach number. In this region, the average value of undisturbed pressure signals is employed to estimate the peak Mach number upstream of the shock wave. In subsonic interactions, the peak Mach numbers at $\eta = 15$ and 17 deg are considerably lower with the upstream blowing jet, shown in Fig. 6a. At $M = 0.83$, even small amounts of blowing jet (smaller B) reduce the peak Mach number. At higher blowing rates, the peak Mach numbers approach the levels without the upstream blowing jet, seen in Fig. 6b. Furthermore, Inger and Babinsky [14] indicated that the mass flow through a plate hole is associated with the hole diameter and plate thickness. Results of the peak Mach number are replotted with the blowing parameter B_d, shown in Fig. 7. For both perforated plates, higher blowing rates result in increasing peak Mach number in transonic interactions, and an opposite trend is observed in subsonic interactions. The porosity effect is more pronounced for separated flows ($M = 0.83$, $\eta = 15$ and 17 deg).

B. Surface Pressure Fluctuations

To further understand the effects of the upstream blowing jet on convex-corner flows, examples of surface pressure fluctuation

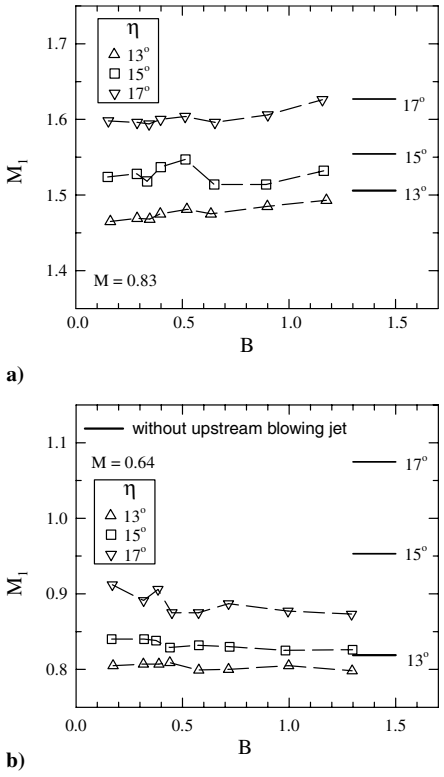

Fig. 6 Peak Mach number, *B* effect.

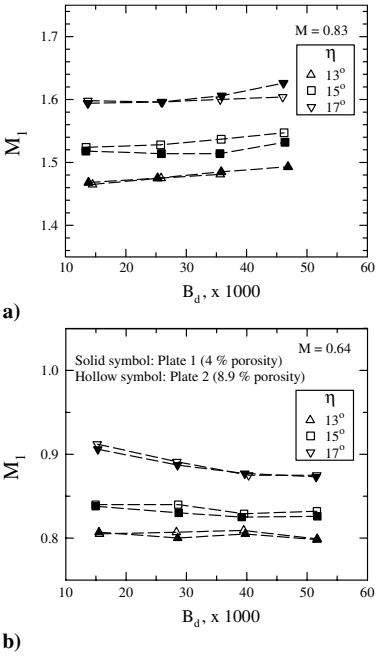

Fig. 7 Peak Mach number, B_d effect.

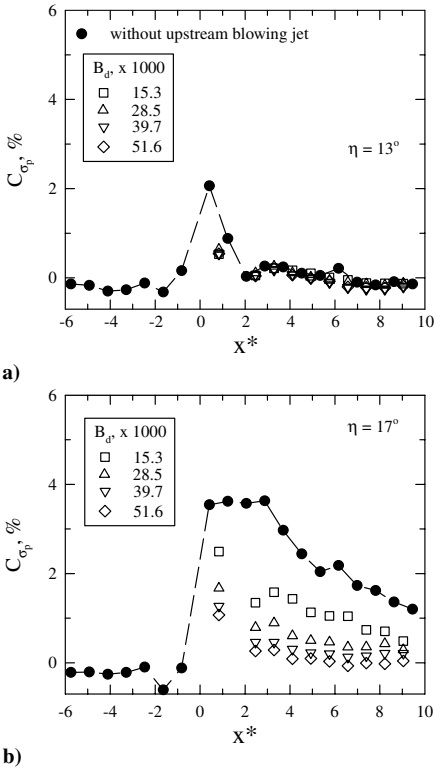

Fig. 8 Pressure fluctuation distributions, $M = 0.64$ (plate 1, 4% porosity).

distribution at $M = 0.64$ are shown in Fig. 8. The pressure fluctuation coefficient (C_{σ_p}) represents the local wall pressure fluctuations normalized by the freestream dynamic pressure (q_∞) with respect to undisturbed flows ($\sigma_{p,\infty}/q_\infty$). For the subsonic expansion flow ($\eta = 13$ deg), the pressure fluctuations increase upstream of the convex corner and reach the maximum immediately downstream of the corner followed by a sharp decrease. The rise in pressure fluctuations corresponds to the initial compression (adverse pressure gradient) downstream of the corner [4]. With the upstream blowing jet, there is a reduction in pressure fluctuations near the corner, shown in Fig. 8a. This is considered due to the decreasing local Mach number [15]. It is also noted that the effect of the blowing rate is not significant. At $\eta = 17$ deg (Fig. 8b), this corresponds to the transition of subsonic and transonic expansion flows. The pressure fluctuations downstream of the corner are considerably higher than the subsonic expansion flows and decrease gradually. With higher levels of B_d, the upstream blowing jets result in a decrease in peak pressure fluctuations near the corner. The amplitude of pressure fluctuations approaches some equilibrium level more quickly with higher blowing rates, which is consistent with the observation of mean surface pressure distributions. This implies that the upstream blowing jet tends to reduce the extent of interaction. At $M = 0.83$ and $\eta = 13$ deg (Fig. 9a), small amounts of upstream blowing jet increase the levels of downstream pressure fluctuations. The effect is less pronounced with increasing B_d. At $\eta = 17$ deg (Fig. 9b), the rapid rise in pressure fluctuations upstream of separation and higher downstream pressure fluctuations are common features of many shock wave/turbulent boundary layer interactions [16]. The upstream blowing jet induces upstream movement of the shock wave. Smaller blowing rates reduce the peak pressure fluctuations while intense large-amplitude fluctuations are associated with larger blowing rates. Furthermore, the porosity effect on the characteristics of pressure fluctuations is also of interest. In transonic interactions, higher porosity (8.9% porosity) tends to decrease peak pressure fluctuations. The reduction is more pronounced for the separated flow at higher blowing rates.

Peak pressure fluctuations are associated with the intermittency of interactions and can be used as an indicator of flow unsteadiness. For the convex-corner flow, the amplitude of peak pressure fluctuations $C_{\sigma_p,\max}$ increases with $M^2\eta$. In subsonic interactions ($M = 0.64$, Fig. 10b), the peak pressure fluctuations with upstream blowing jet are considerably smaller. The effect of injection rates is more significant at a higher convex-corner angle. This is considered due to the variation in local Mach numbers, seen in Fig. 7. At $M = 0.83$, small amounts of upstream blowing jet exert a beneficial influence on the unsteadiness of the flow, seen in Fig. 10a. Peak pressure fluctuations reach the minimum at $B \approx 0.5$ for all the test cases. Higher blowing rates have a minor influence at $\eta = 13$ deg, and have an adverse effect in hastening the intermittency (or shock excursion) at $\eta = 15$ and 17 deg. In addition, the porosity effect on the

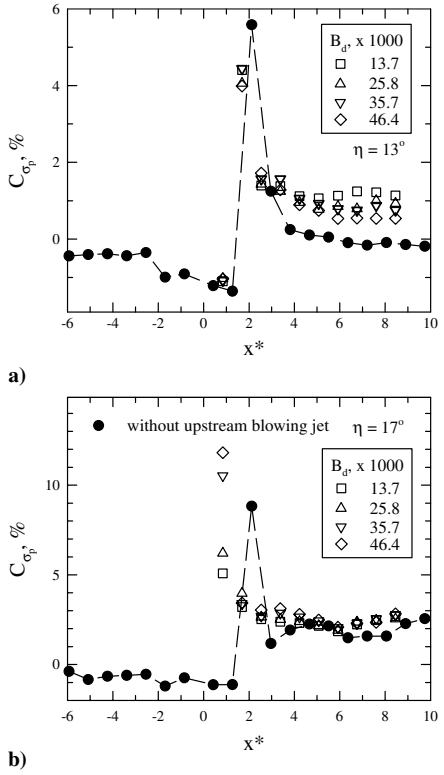

Fig. 9 Pressure fluctuation distributions, $M = 0.83$ (plate 1, 4% porosity).

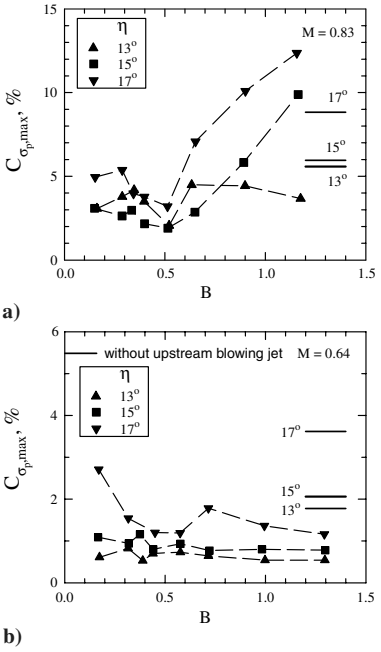

Fig. 10 Peak pressure fluctuations, *B* effect.

intermittency is also of primary concerns. The data of peak pressure fluctuations are replotted in Fig. 11. As can be seen, porosity at a given blowing rate has a minor influence on the amplitude of peak pressure fluctuations in subsonic interactions, shown in Fig. 11b, which is similar to the variations in peak Mach number with porosity (Fig. 7b). At $M = 0.83$ and $\eta = 13$ deg, there is a slight variation in the peak pressure fluctuations with B_d for both perforated plates. At a given B_d, the intense peak pressure fluctuations are associated with higher porosity (plate 2, 8.9% porosity). For the extensively separated flow ($\eta = 15$ and 17 deg), the porosity effect is significant. The surface pressure is highly intermittent with higher porosity at relatively larger blowing rates.

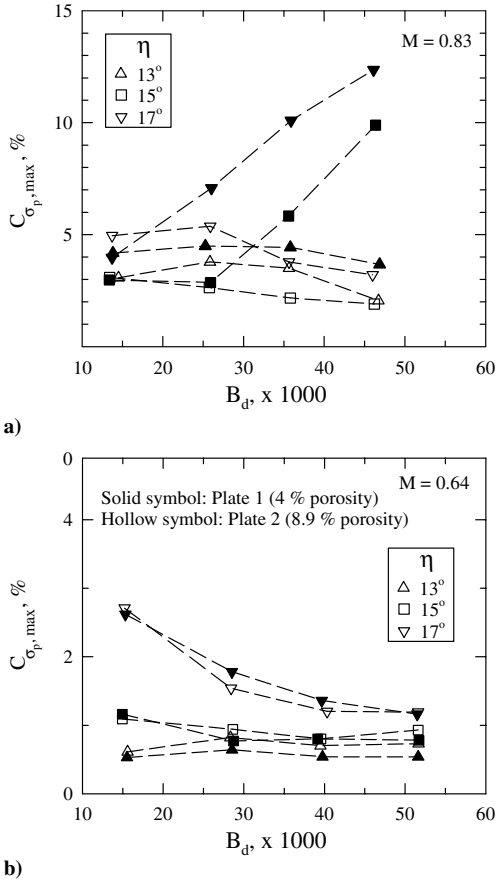

Fig. 11 Peak pressure fluctuation coefficients, B_d effect.

IV. Conclusions

The present study investigates the compressible convex-corner flows with upstream blowing jet. The effects of porosity and blowing rate on subsonic and transonic interactions are summarized here.

1) The upstream blowing jet results in less expansion near the convex corner in subsonic interactions, which are associated with the delay in transition of the subsonic and transonic expansion flows. Decreasing peak pressure fluctuations are related to the local peak Mach number.

2) In transonic interactions ($M^2\eta = 8.96$), there are limited effects of blowing rate and porosity on the mean and fluctuating pressure distributions. However, the upstream blowing jet induces stronger adverse pressure gradient near the corner with increasing injection rates (B_d). There is a slight increase in peak Mach number with higher blowing rates (B_d), which also increase the levels of downstream pressure fluctuation.

3) The porosity has a significant effect on the large-amplitude disturbance and shock location for separated flows. Larger amounts of blowing result in upstream movement of the shock wave and enhance the intermittency.

Acknowledgments

The research was supported by the National Science Council under grant NSC 95-2212-E-006-065-MY3. The authors would like to thank the technical support of Aerospace Science and Technology Research Center/National Cheng-Kung University (ASTRC/NCKU) technical staffs with the experiments.

References

[1] Bolonki, A., and Gilyard, G. B., "Estimated Benefits of Variable-Geometry Wing Camber Control for Transport Aircraft," NASA TM-1999-206586, Oct. 1999.

[2] Mason, W. H., "Fundamental Issues in Subsonic/Transonic Expansion Corner Aerodynamics," AIAA Paper 93-0649, Jan. 1993.

[3] Chung, K., "Transition of Subsonic and Transonic Expansion Flows," *Journal of Aircraft*, Vol. 37, No. 6, 2000, pp. 1079–1082.
[4] Chung, K., "Unsteadiness of Transonic Convex-Corner Flows," *Experiments in Fluids*, Vol. 37, No. 6, 2004, pp. 917–922. doi:10.1007/s00348-004-0890-3
[5] Chung, K., "Investigation on Transonic Convex-Corner Flows," *Journal of Aircraft*, Vol. 39, No. 6, 2002, pp. 1014–1018.
[6] Wong, W. F., and Hall, G. R., "Suppression of Strong Shock Boundary Layer Interaction in Supersonic Inlets by Boundary Layer Blowing," AIAA Paper 75-1209, Sept. 1975.
[7] Inger, G. R., and Zee, S., "Transonic Shockwave/Turbulent Boundary Layer Interaction with Suction or Blowing," *Journal of Aircraft*, Vol. 15, No. 11, 1978, pp. 750–754.
[8] Fernandez, F. L., and Zukoski, E. E., "Experiments in Supersonic Turbulent Flow with Large Distributed Surface Injection," *AIAA Journal*, Vol. 7, No. 9, 1969, pp. 1759–1767.
[9] Chung, K., "Development and Calibration of ASTRC/NCKU 600 mm × 600 mm Transonic Wind Tunnel," NSC 83-2212-E-006-141T, Taiwan, Aug. 1994.
[10] Gramann, R. A., and Dolling, D. S., "Detection of Turbulent-Boundary Layer Separation Using Fluctuating Wall Pressure Signals," *AIAA Journal*, Vol. 28, No. 6, 1990, pp. 1052–1056.
[11] Miau, J., Cheng, J., Chung, K., and Chou, J., "The Effect of Surface Roughness on the Boundary Layer Transition," *Proceedings of the 7th International Symposium in Flow Modeling and Turbulent Measurement, ISFMTM98'*, National Cheng Kung University, Tainan, Taiwan, 1998, pp. 609–616.
[12] Valki, A. D., Wolfe, R., Nagle, T., and Lambert, E., "Active Control of Cavity Aeroacoustics in High Speed Flows," AIAA Paper 95-0678, Jan. 1995.
[13] Liu, X., and Squire, L. C., "An Investigation of Shock/Boundary Layer Interactions on Curved Surfaces at Transonic Speeds," *Journal of Fluid Mechanics*, Vol. 187, Feb. 1988, pp. 467–486. doi:10.1017/S0022112088000527
[14] Inger, G. R., and Babinsky, H., "Viscous Compressible Flow Across a Hole in a Plate," AIAA Paper 99-3139, June 1999.
[15] Lagnelli, A. L., Martellucci, A., and Shaw, L. L., "Wall Pressure Fluctuations in Attached Boundary Layer Flows," *AIAA Journal*, Vol. 21, No. 4, 1983, pp. 495–502.
[16] Dolling, D. S., "Fifty Years of Shock Wave/Boundary Layer Interaction research: What Next?," *AIAA Journal*, Vol. 39, No. 8, 2001, pp. 1517–1531.